

Radar-Assisted Beam Management Framework for mmWave NTN: Overhead Reduction and Physical Layer Security Application

Bora Bozkurt^{*§}, Cevdet Tosun^{*§}, Mehmet Nuri Akıncı[§],
Ali Gorcin^{*§}, Ibrahim Hokelek^{*}, Mehmet Kemal Özdemir[¶]

^{*}Communications and Signal Processing Research (HİSAR) Lab., TÜBİTAK BİLGEM, Kocaeli, Türkiye

[§]Department of Electronics and Communication Engineering, Istanbul Technical University, İstanbul, Türkiye

[¶]Department of Electrical and Electronics Engineering, Medipol University, İstanbul, Türkiye

Abstract—Fast and low-overhead beam management is a critical requirement for the practical deployment of non-terrestrial networks (NTNs) operating at millimeter-wave and higher frequencies. In this paper, we propose a radar-assisted beam selection framework for NTNs that limits the set of candidate beams by utilizing spatial sensing information such as the angle-of-departure (AoD) and distance estimations. To provide theoretical insight into the expected worst-case overhead, we conduct a probabilistic analysis under idealized conditions, where an approximation of the worst-case beam selection overhead is proposed and its statistics are derived under Gaussian error. Additionally, the proposed framework is applied to a physical-layer security (PLS) scenario by leveraging the radar’s capability to detect passive targets that represent unintended users. The simulation results show that the unintended user’s power is suppressed below -135 dBm, while an additional beamforming gain of roughly 2 dB is attained for the legitimate users.

Index Terms—ISAC, sensing-assisted, radar, beamforming, beam selection, NTN.

I. Introduction

Integrated sensing and communication (ISAC) presents unprecedented opportunities in wireless networks as a key concept for enabling next generation applications and services [1]. The promise of ISAC stems from significant gains such as reduced hardware costs, improved spectral efficiency, and lower energy consumption achieved through efficient integration of communication and sensing functionalities. The concept of ISAC that specifically addresses the problem of improving communication system performance using the sensing information is called sensing-assisted communication (SAC) [2]. The studies on SAC have mostly focused on optimizing beamforming using the sensing information for essentially improving the performance of millimeter-wave (mmWave) and sub-THz communications [2]. In practice, many SAC implementations rely on shared hardware or loosely coupled sensing and communication chains rather than full waveform-level integration [2]. Given the challenges associated with joint signaling and processing, a practical approach is to design sensing and communication waveforms independently and implement them using separate baseband processing chains.

In SAC systems with a dedicated sensing assistance, machine learning (ML) or more generally artificial intelligence (AI) has emerged as a widely adopted approach for beam management¹. The survey by Brillhante et al. illustrates this landscape extensively [3]. It should be noted that recent studies have also explored fusion-based techniques for predicting the best beams from multi-modal data, for which an example is given in [4]. The need for such sophisticated AI-based techniques is due to the highly non-linear relationship between the optimal beams and the sensing data, induced by a channel with complex scattering conditions.

Unlike terrestrial networks, non-terrestrial networks (NTNs) typically operate within a line-of-sight (LoS) dominated channel [5], which make structured and model-based beam management approaches particularly attractive. Hence, sensing-assisted beamforming and beam management studies for NTNs mostly follow analytical formulations. A comprehensive study by Yanpeng et al. [6] developed a beam management framework for mmWave drone networks that utilizes echoed communication signals alongside visual information at the base station (BS). The authors suggested a solution for user identification that matches the users’ physical information with their temporary identifiers so that the beams can be allocated to their intended users. Benaya et al. [7] proposed a secure NTN architecture with a high-altitude platform station (HAPS) mounted ISAC BS and studied optimizing the sum spectral efficiency and secrecy rate of the system through beamforming and jamming. The scenario of sensing-assisted joint trajectory and beamforming optimization was investigated in [8], [9]. Finally, Chen et al. [10] studied sensing-assisted beam tracking and beamwidth control suitable for unmanned aerial vehicle (UAV) communications. For tracking the target’s motion path and optimizing the average achievable rate, they leveraged the sensing information with a motion path

¹“Beam management” is an umbrella term that refers to any process used for optimizing the beam choice from a predefined codebook. This includes (initial) beam selection and beam tracking.

model at the BS.

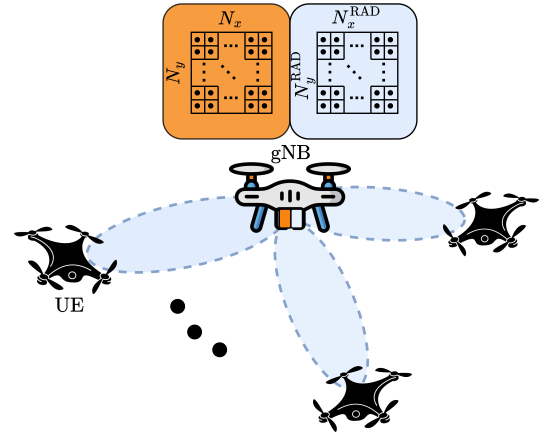
Despite these efforts, sensing-assisted beam management for NTN remains relatively underexplored, particularly for the initial access stage and for architectures relying solely on radar as the sensing modality. Motivated by this gap, this paper proposes a novel radar-assisted beam selection framework for the initial access stage of NTN. In contrast to [6], the proposed approach relies exclusively on radar for sensing assistance. In addition, the distance information provided by the radar is utilized to impose an early stopping condition based on the received power feedback so that the beam selection complexity is further reduced. The main contributions of this paper are summarized as follows:

- We propose a radar-assisted beam selection framework for NTN initial access, where the radar first identifies coarse target directions and the communication array then performs narrow-beam sweeping only within the detected regions. Within the framework, we introduce a distance-aware early stopping criterion based on radar-estimated UE range and received power feedback, reducing beam search overhead while preserving narrow communication beams and low RF-chain complexity.
- An analysis on the worst case beam selection overhead probability under a suboptimal beam search strategy is provided. More specifically, via simplifying ideal assumptions, we present an approximation for the worst case overhead and characterize its statistics under Gaussian estimation error.
- Leveraging the fact that the radar can detect passive targets that are potentially eavesdroppers, the proposed scheme is further extended for physical layer security (PLS) application. The performance of this security application is evaluated through comprehensive simulations.

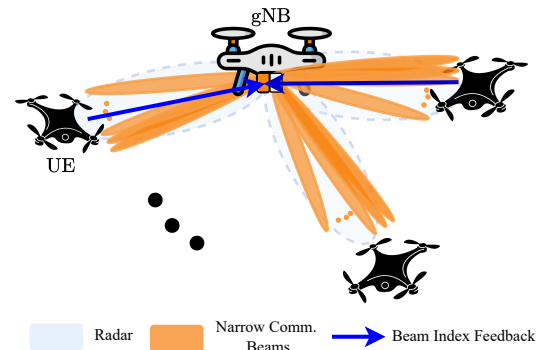
II. System Model

We consider a non-terrestrial SAC system, where an aerial 5G mmWave BS (gNB) equipped with two co-located uniform rectangular arrays (URAs) serve aerial user equipments (UEs). As illustrated in Fig. 1a, one of the URAs is designated for the radar function of the gNB while the other is used for providing communication with the UEs. The NTN channel allows the radar to capture accurate spatial information about the users and other passive targets. After detecting all potential UEs using the radar, the codebook-based beam selection procedure is conducted². Since the beam selection is handled separately at UEs and gNBs in practical systems [11], we deal with the gNB side only and assume that there is a single antenna at UEs. Specifically, the gNB selects a beam for

²Technically, beam selection refers to identifying a certain set of beams from the codebook that are potentially the best, whereas beam training is the process used to select the best beam out of this set. However, in this paper, we refer to this whole process as beam selection to avoid conceptual confusion.



(a) The system model with aerial gNB and UEs, where the radar performs coarse target detection using wide digital beams.



(b) The communication array refines the radar's coarse estimate via narrow analog beam sweeping.

Fig. 1: The radar-assisted beam selection framework.

each UE by observing the beam index feedback, which is determined by the UE from the received signal reference power (RSRP) values.

Let the URA of the gNB used for communication be of size $N_x \times N_y$, where $N_x, N_y \geq 2$ and $N_A = N_x N_y$, with inter-element spacing equal to half-wavelength for both axes. Define the normalized symbol transmitted by the gNB to the UE with $s \in \mathbb{C}, |s| = 1$. At the t^{th} time slot ($t = 1, \dots, T$), the symbol is multiplied with a weight vector, i.e., beam, $\mathbf{f}[t] \in \mathcal{F}$, belonging to the codebook \mathcal{F} . Consistent with the beam refinement procedure in 5G NR, we use an oversampled 2D discrete time Fourier transform (DFT) codebook [11] with integer oversampling factor $O \geq 1$. Prior to defining the codebook, we introduce the normalized DFT vector

$$\mathbf{w}_N(k) = \frac{1}{\sqrt{N}} \left[1, e^{-j\pi\mu_N(k)}, \dots, e^{-j\pi(N-1)\mu_N(k)} \right]^T, \quad (1)$$

where $\mu_N(k) = 2k/(ON) - 1$ represents the sine domain steering angle. Using (1) and the Kronecker product

operator \otimes , the codebook is written as

$$\mathcal{F} = \{\mathbf{w}(k, m) = \mathbf{w}_{N_x}(k) \otimes \mathbf{w}_{N_y}(m) : k \in \{1, \dots, ON_x\} \text{ and } m \in \{1, \dots, ON_y\}\}. \quad (2)$$

After multiplication with the weight vector, the signal is transmitted through the channel and received at the UE as

$$y[t] = \sqrt{P}\mathbf{h}^T \mathbf{f}[t]s + n[t], \quad (3)$$

where P is the transmission power, $\mathbf{h} \in \mathbb{C}^{N_A \times 1}$ denotes the narrowband flat fading channel, which is assumed to be constant during the beam selection period, and $n[t] \sim \mathcal{CN}(0, \sigma^2)$ is the additive white Gaussian noise distributed independently with respect to (w.r.t.) t . Finally, the achievable rate of the UE at time slot t is given by

$$R[t] = \log_2(1 + \text{SNR}[t]) = \log_2\left(1 + \frac{P|\mathbf{h}^T \mathbf{f}[t]|^2}{\sigma^2}\right). \quad (4)$$

We model the mmWave channel with the widely considered geometric channel model and use Rician fading with L paths as in [6], [7]. The dominant angle of departure (AoD) for the UE is shown with the azimuth-elevation angle pair $(\phi, \theta) \in [-\pi/2, \pi/2]^2$. Similarly, the AoDs of the scattered components are denoted by (ϕ_ℓ, θ_ℓ) , $\ell = 1, \dots, L-1$. Consequently, the UE's channel is represented by

$$\mathbf{h} = \sqrt{\frac{N_A}{L}} \left(\sqrt{\frac{K}{K+1}} \beta \mathbf{a}(\phi, \theta) + \sqrt{\frac{1}{K+1}} \sum_{\ell=1}^{L-1} \alpha_\ell \mathbf{a}(\phi_\ell, \theta_\ell) \right), \quad (5)$$

where K is the Rician K -factor, β is the dominant path's loss factor, $\alpha_\ell \sim \mathcal{CN}(0, \sigma_\ell^2)$ is the complex path gain of the ℓ^{th} scattered component, and

$$\mathbf{a}(\phi, \theta) = \frac{1}{\sqrt{N_A}} \left[1, e^{j\pi \cos(\phi) \sin(\theta)}, \dots, e^{j(N_x-1)\pi \cos(\phi) \sin(\theta)} \right]^T \otimes \left[1, e^{j\pi \sin(\phi) \sin(\theta)}, \dots, e^{j(N_y-1)\pi \sin(\phi) \sin(\theta)} \right]^T \quad (6)$$

denotes the azimuth-elevation URA steering vector for half wavelength spacing and isotropic elements. For conversion between sine and angle domains, we also define the mapping ψ from $[-\pi/2, \pi/2]^2$ into the unit disk $\mathbb{D} \subset \mathbb{R}^2$ as

$$\psi = (\phi, \theta) \mapsto (\cos(\phi) \sin(\theta), \sin(\phi) \sin(\theta)). \quad (7)$$

III. Proposed Radar-assisted Beam Selection Framework

The proposed radar-assisted beam selection framework, which is shown in Fig. 1, aims to skip the initial beam sweeping procedure by utilizing wider beams generated by the radar and directly performs beam refinement using the narrower DFT beams. To this end, for each UE, the gNB uses its radar to roughly estimate the (dominant) AoD and the distance of the UE bearing this AoD. As in [6], we assume that the gNB is able to determine which spatial information (AoD and distance) belongs to which UE by pairing the UEs' spatial information with their temporary

identifiers assigned by the network. In this paper, we do not consider the identity matching problem and refer the interested readers to [6].

Once the AoD of a UE, $(\hat{\phi}, \hat{\theta})$, is estimated with the radar, the gNB performs a sweep using the appropriate subset of the codebook \mathcal{F} to select the best beam maximizing the received power, and therefore the achievable rate by (4). We define this subset, $\mathcal{C} \subset \mathcal{F}$, as the set of codebook elements whose sine domain steering angle is included in the rectangle $D = [\hat{\varphi}_{\min}, \hat{\varphi}_{\max}] \times [\hat{\vartheta}_{\min}, \hat{\vartheta}_{\max}]$. The center of this rectangle is the estimated sine domain AoD $(\hat{\varphi}, \hat{\vartheta}) = \psi(\hat{\phi}, \hat{\theta})$. Here, D represents the coarse region detected for the UE by the radar. Consequently, the codebook is written as

$$\mathcal{C} = \{\mathbf{w}(k, m) \in \mathcal{F} : (\mu_{N_x}(k), \mu_{N_y}(m)) \in D\}. \quad (8)$$

Apart from the AoD, the gNB also makes use of the estimated distance, \hat{d} , of the UE to further reduce selection overhead. Using this distance information, the gNB is able to approximate a threshold value, $P_{\text{th}} \leq P$, for the received signal power. In traditional beam selection, the optimal beam index maximizing received power is feedback to the gNB by the UE after all the candidate beams are tested. In our proposed scheme, the gNB utilizes the threshold P_{th} to enforce an early stopping condition for the beam sweep. To achieve this, prior to beam selection, the gNB transmits the pre-determined P_{th} value to the UE. As the beams are swept, the UE signals to the gNB through the feedback channel to stop, when a certain beam yields a received power greater than or equal to P_{th} . The beam that triggered the stopping condition is then selected for that specific UE. In contrast to the traditional method, this mechanism requires an extra feedback task on the UE side to check if the stopping criterion is satisfied or not. However, this disadvantage becomes insignificant when the stopping condition is met sufficiently early, leading to a significant reduction in overhead.

For the sake of clarity, the beam selection scheme can be formally described as follows. Let the time index t denote an arbitrary ordering of the codebook elements as

$$\mathbf{f}[1] = \mathbf{w}(k[1], m[1]), \dots, \mathbf{f}[T] = \mathbf{w}(k[T], m[T]), \quad (9)$$

where $T = |\mathcal{C}|$ represents the number of elements in the set \mathcal{C} . Then, the optimal beam index maximizing the rate considering the whole codebook is

$$\tau_{\text{opt}} = \underset{1 \leq t \leq T}{\text{argmax}} R[t] = \underset{1 \leq t \leq T}{\text{argmax}} \left| \mathbf{h}^T \mathbf{f}[t] \right|^2. \quad (10)$$

On the other hand, according to the stopping condition previously described, the gNB selects the beam index

$$\tau = \min \left\{ t \in \{1, \dots, T\} : \left| \mathbf{h}^T \mathbf{f}[t] + n[t] \right|^2 \geq P_{\text{th}} \right\}. \quad (11)$$

If the set on the right hand side of (11) is empty, then the gNB simply selects the index of the beam maximizing the received power. A natural choice for the value of P_{th}

is $\alpha P\beta^2 N_A$, where $\alpha \in (0, 1)$ is a tunable constant and $P\beta^2 N_A$ is the maximum power that can be attained for a single path channel. Note that the path loss factor β can be derived from the estimated UE distance in possession of the gNB using the free-space path loss formula.

IV. Analysis of Worst Case Beam Selection Overhead Probability

This section presents an analysis on the beam selection overhead probability w.r.t. a distance based search strategy. The overhead induced by this strategy is termed as the "worst case overhead" given the strategy's naive and obviously suboptimal nature. To set the stage, we first introduce some preliminary assumptions which allow us to analyze the worst case overhead w.r.t. the unique early stopping mechanism of our scheme in a tractable setting. Firstly, we confine our analysis to a high SNR scenario with no noise and fix the channel to a single path, i.e., $\mathbf{h} = \beta\sqrt{N_A}\mathbf{a}(\phi, \theta)$. Furthermore, it is assumed that the path loss constant β is estimated perfectly from the UE's distance. Note that the single path assumption is reasonable for an NTN scenario. Secondly, we set $P_{\text{th}} = P\alpha\beta^2 N_A$ and assume that there always exists a beam $\mathbf{f}[t] \in \mathcal{C}$ such that $|\mathbf{h}^T \mathbf{f}[t]|^2 \geq P_{\text{th}}$. The latter can be justified with the high granularity of the oversampled DFT codebook. Finally, we assume that α is sufficiently close to 1 so that $|\mathbf{h}^T \mathbf{f}[t]| \geq P_{\text{th}} \iff t = \tau_{\text{opt}}$. Recall that $(\hat{\varphi}, \hat{\vartheta}) = \psi(\hat{\phi}, \hat{\theta})$ and $(\varphi, \vartheta) = \psi(\phi, \theta)$ denote the sine domain AoD estimated by the radar and the actual sine domain AoD, respectively. These assumptions imply that

$$\tau = \tau_{\text{opt}} \iff (\varphi, \vartheta) \in D[t] \quad (12)$$

where

$$D[t] = \left[\mu_{N_x}(k[t]) - \frac{1}{ON_x}, \mu_{N_x}(k[t]) + \frac{1}{ON_x} \right] \times \left[\mu_{N_y}(m[t]) - \frac{1}{ON_y}, \mu_{N_y}(m[t]) + \frac{1}{ON_y} \right]. \quad (13)$$

Note that the equivalence in (12) follows from the uniformly spaced structure of the DFT beams. The relation $\tau = \tau_{\text{opt}}$ enables us to neglect beam misalignment, simplifying the analysis. In this scenario, the selection overhead becomes purely influenced by the radar's estimation error and the order of the codebook beams. For a more general treatment involving misalignment probability, the readers are referred to [12]. Finally, we note that with these assumptions, it is ensured that the true AoD always belongs to the region detected by the radar, i.e., $(\varphi, \vartheta) \in D \subset \bigcup_{t=1}^T D[t]$. This is reasonable given that D is large and the estimation error is typically small.

A. WCOA for Naive Distance Based Strategy

We now derive the worst case overhead approximation (WCOA) under the aforementioned assumptions. Modeling the sine domain estimation error along both axes with

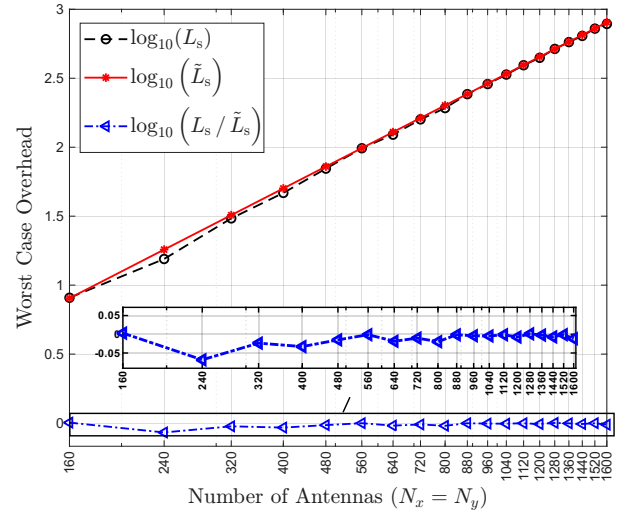


Fig. 2: Values of L_s and \tilde{L}_s w.r.t. $N = N_x = N_y$.

the random variables δ_x and δ_y , we get $\hat{\varphi} = \varphi + \delta_x$ and $\hat{\vartheta} = \vartheta + \delta_y$. Consequently, the total euclidean error of the estimated AoD becomes

$$\delta = \sqrt{(\hat{\varphi} - \varphi)^2 + (\hat{\vartheta} - \vartheta)^2} = \sqrt{\delta_x^2 + \delta_y^2}. \quad (14)$$

Various efficient closed-loop techniques have been proposed for estimating the true AoD and hence the best beam by utilizing the received power values. However, for the sake of tractability and to focus on the worst case, here we adopt a naive distance based search strategy, which can be seen as a suboptimal benchmark. According to this strategy, the beams are ordered such that the distance between the sine domain steering angle of $\mathbf{f}[t]$ and the estimated AoD $(\hat{\varphi}, \hat{\vartheta})$ is non-decreasing w.r.t. t . As can be observed from (12), this implies that a search over the nearest rectangles, $D[1], D[2], \dots$, around the estimated AoD is conducted, until the condition $|\mathbf{h}^T \mathbf{f}[t]|^2 \geq P_{\text{th}} \iff t = \tau = L_s \iff (\varphi, \vartheta) \in D[L_s]$ is met. Here, L_s denotes the worst case overhead. Let $\mathcal{D} = \bigcup_{t=1}^{L_s} D[t]$. Since all rectangles $D[t]$ have equal area, we have

$$L_s = \frac{A(\mathcal{D})}{A(D[1])} = \frac{O^2 N_x N_y A(\mathcal{D})}{4}, \quad (15)$$

where A is the set function that yields the total area of a rectangle in \mathbb{R}^2 . In our scenario, the DFT beams used for communication have a small beam width, thus we consider the case where ON_x and ON_y are large enough so that $r = \sqrt{(2/(ON_x))^2 + (2/(ON_y))^2} < \delta$. For a given realization of δ , it is clear that $B((\hat{\varphi}, \hat{\vartheta}), \delta - r) \subset \mathcal{D} \subset B((\hat{\varphi}, \hat{\vartheta}), \delta + r)$, where $B((\hat{\varphi}, \hat{\vartheta}), \delta \pm r) \subset \mathbb{R}^2$ is the ball with center $(\hat{\varphi}, \hat{\vartheta})$ and radius $\delta \pm r$. Hence,

$$\begin{aligned} A(B((\hat{\varphi}, \hat{\vartheta}), \delta - r)) &\leq A(\mathcal{D}) \leq A(B((\hat{\varphi}, \hat{\vartheta}), \delta + r)) \\ \iff \pi(\delta - r)^2 &\leq A(\mathcal{D}) \leq \pi(\delta + r)^2 \\ \iff \frac{O^2 N_x N_y \pi(\delta - r)^2}{4} &\leq L_s \leq \frac{O^2 N_x N_y \pi(\delta + r)^2}{4} \end{aligned} \quad (16)$$

from the monotonicity of the set function A and (15). Furthermore, as $N_x, N_y \rightarrow \infty$, we get $r \rightarrow 0$, implying

$$\lim_{N_x, N_y \rightarrow \infty} \frac{4L_s}{O^2 N_x N_y \pi \delta^2} = 1 \quad (17)$$

from (16). Finally, using (17) and the bounds in (16), we obtain the suggested WCOA

$$L_s \approx \tilde{L}_s = \frac{O^2 N_x N_y \pi \delta^2}{4}. \quad (18)$$

To illustrate the accuracy of the approximation, Fig. 2 shows the numerical results of the actual worst case overhead L_s and the WCOA \tilde{L}_s . For these results, we set $O = 1$, $(\hat{\varphi}, \hat{\vartheta}) = \psi(\pi/3, \pi/3)$, and distribute (φ, ϑ) uniformly on a circle such that the Euclidean distance between the actual AoD (φ, ϑ) and the estimated AoD $(\hat{\varphi}, \hat{\vartheta})$ is equal to δ . In addition, we fix $\delta = 0.2$, thus $r < \delta$ for all array configurations. Fig. 2 shows that the approximation \tilde{L}_s follows L_s accurately over a wide range of antenna numbers.

B. Statistics of the WCOA for Gaussian Error

In order to find the statistics of the approximation \tilde{L}_s , we need the statistics of δ^2 . Consider independent zero mean Gaussian error along both axes, i.e., $\delta_x \sim \mathcal{N}(0, \zeta_x^2)$ and $\delta_y \sim \mathcal{N}(0, \zeta_y^2)$. It follows that $\delta^2 = \delta_x^2 + \delta_y^2$ has a squared Hoyt distribution [13], whose probability density function (PDF) is written as

$$f_{\delta^2}(z) = \begin{cases} \frac{1+q^2}{2q\gamma} \exp\left(-\frac{(1+q^2)^2 z}{4q^2\gamma}\right) I_0\left(\frac{(1-q^4)z}{4q^2\gamma}\right), & z \geq 0, \\ 0, & z < 0, \end{cases} \quad (19)$$

where I_0 is the modified Bessel function of the first kind and order zero, $\gamma = E[\delta^2] = \zeta_x^2 + \zeta_y^2$ and $q = \zeta_x^2/\zeta_y^2$ for $\zeta_x^2 \geq \zeta_y^2$. Assuming that $\zeta_x^2 = \zeta_y^2 = \zeta^2$, and hence $\gamma = 2\zeta^2$, δ^2 becomes an exponential random variable [13] and its PDF simplifies to

$$f_{\delta^2}(z) = \begin{cases} \frac{1}{2\zeta^2} \exp\left(-\frac{z}{2\zeta^2}\right), & z \geq 0, \\ 0, & z < 0. \end{cases} \quad (20)$$

Therefore, utilizing (18) and (20), in the case of equal variances, the PDF of \tilde{L}_s can be expressed as

$$\begin{aligned} f_{\tilde{L}_s}(z) &= \frac{4}{O^2 N_x N_y} f_{\delta^2}\left(\frac{4z}{O^2 N_x N_y}\right) = \\ &= \begin{cases} \frac{2}{O^2 N_x N_y \zeta^2} \exp\left(-\frac{2z}{O^2 N_x N_y \zeta^2}\right), & z \geq 0, \\ 0, & z < 0, \end{cases} \end{aligned} \quad (21)$$

with mean $E[\tilde{L}_s] = O^2 N_x N_y \zeta^2 / 2$ and variance $\text{var}[\tilde{L}_s] = (O^2 N_x N_y \zeta^2 / 2)^2$. Similarly, one can derive the PDF of \tilde{L}_s in the case of unequal variances using (18) and (19).

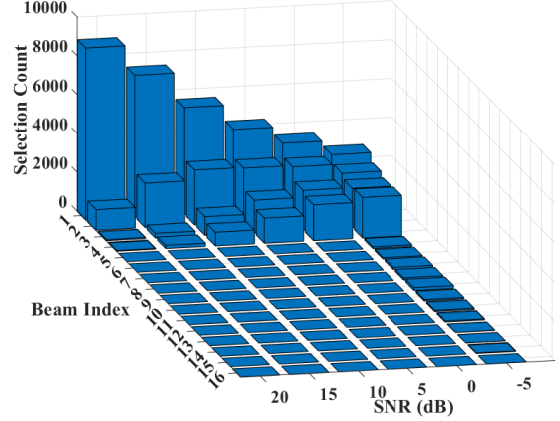


Fig. 3: 3D distribution of beam indices across different SNRs.

V. Enhancing PLS Using Radar Information

As previously explained in Section III, the gNB is able to match the UEs' spatial information with their temporary network identifiers. In doing so, the gNB must also acknowledge the spatial information of the detected passive targets that do not correspond to legitimate UEs. With this knowledge at hand, the gNB can modify its beams to ensure that these passive targets, i.e., unintended users, are not able to capture the communication signal effectively. Suppose that the dominant AoDs of the unintended users are estimated as $(\bar{\phi}_1, \bar{\theta}_1), \dots, (\bar{\phi}_N, \bar{\theta}_N)$. The gNB then takes these channels to be $\bar{\mathbf{h}}_i = \mathbf{a}(\bar{\phi}_i, \bar{\theta}_i)$ owing to the NTN channel. Suppose that the beam \mathbf{f} is selected, the gNB can now use regularized zero forcing [14] to null this beam in the unintended users' directions via $\tilde{\mathbf{f}} = \mathbf{f}_{\text{RZF}} / \|\mathbf{f}_{\text{RZF}}\|$, where

$$\mathbf{f}_{\text{RZF}} = \left(\sum_{i=1}^N \bar{\mathbf{h}}_i \bar{\mathbf{h}}_i^H + \eta \mathbf{I}_{N_A} \right)^{-1} \mathbf{f}. \quad (22)$$

Here, η represent the regularization factor and \mathbf{I}_{N_A} is the $N_A \times N_A$ identity matrix. This technique is utilized to null the unintended user and enhance the beamforming gain.

A. Simulation and Results

The simulation environment consists of a radar-assisted gNB at 500 m altitude and three UEs with -10 dBsm radar cross section, at $x = \{80, 40, 60\}$, $y = \{20, 60, -30\}$, and $z = \{520, 510, 480\}$, respectively. The radar uses a 24 GHz LFM waveform (200 MHz bandwidth, 300 μ s pulse) with an 8×8 URA applying Chebyshev tapering, and MUSIC for high-resolution direction of arrival estimation. The communication subsystem operates at 28 GHz via a 32×32 URA on the gNB UAV, generating highly directive narrow beams. Beam selection leverages radar-based coarse UE locations with a 16-stage sequential codebook search, following a center-to-outward pattern. Range-based path loss estimates are used to set a detection

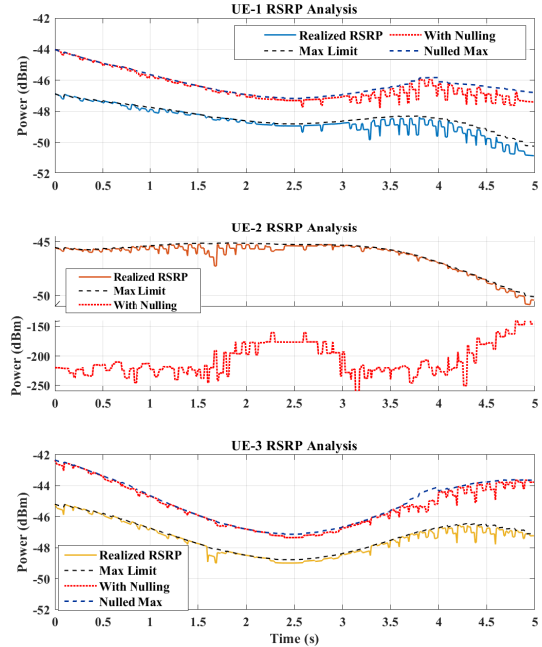
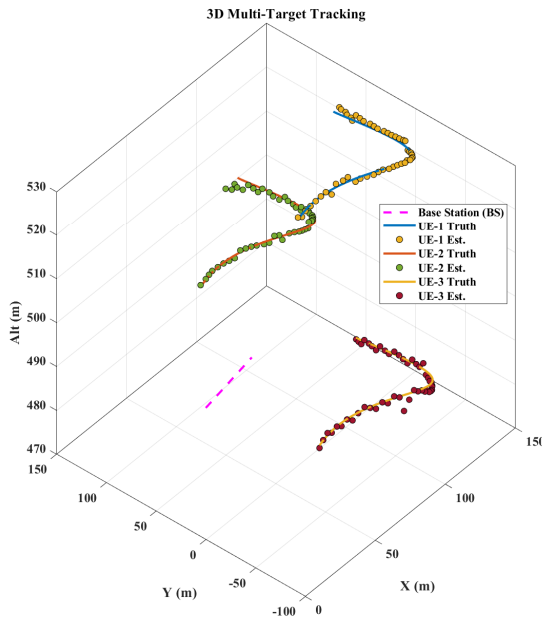


Fig. 4: Tracked UE positions and RSRP plots for the case of no nulling and for the case of nulling UE-2.

threshold 9 dB below the maximum predicted received power; beam index feedback is triggered only for beams exceeding this threshold, and the beam with the highest RSRP establishes the optimal link. To demonstrate the effectiveness of nulling, in the simulation, we use a single beam that serves all users simultaneously according to their spatial information.

Figure 4 displays the 3D plot showing the tracked UE positions along with the BS’s position, and the RSRPs of the UEs for different scenarios at each iteration. In this case, the second UE is deemed as belonging to the unintended network user, and hence the gNB nulls its direction via zero-forcing as in (22). The curves labeled ”realized RSRP” correspond to the case when there is no nulling employed by the gNB. On the other hand, the curves with the label ”with nulling” present the results for the case when the unintended user’s (UE-2) direction is nulled. The dashed lines indicate the maximum attainable RSRP with no radar estimation error for both cases. The results show that, upon nulling the unintended user, the first and third UEs both experience an average RSRP increase of 2.218 and 2.174 dBs, respectively. Furthermore, it is observed that the nulled second UE’s RSRP stays below -135 dBm. These findings demonstrate that the proposed scheme not only improves overall beamforming gain for intended users but also enhances the system’s physical-layer security by effectively suppressing unintended signal leakage.

Secondly, Fig. 3 shows the frequency distribution of selected beam indices for the first UE across different SNR levels. At high SNR (e.g., 20 dB), the distribution is tightly concentrated, with the gNB consistently selecting the

optimal ray index corresponding to the UE’s true spatial location, resulting in received power above the threshold at the first two ray indices. This confirms that beam index feedback based on RSRP provides sufficient resolution for accurate ray alignment in low-noise conditions. As SNR decreases to -5 dB, the histogram broadens due to noise and phase fluctuations, yet the primary mode remains aligned with the target beam, demonstrating the robustness under low-SNR conditions.

VI. Conclusion

In this paper, we put forward a novel radar-assisted beam selection framework with an emphasis on overhead reduction through the efficient use of spatial information obtained by the radar. As a theoretical contribution, we conducted an analysis of the worst case overhead probability, providing a performance benchmark for similar sensing-assisted schemes. Furthermore, we investigated a PLS application within the proposed framework and reported the results from a comprehensive simulation. Overall, with this work, we have provided a viable and low-overhead solution for beam management in practical NTN systems operating at mmWave and higher frequency bands. Future work will consider dynamic environments, hybrid precoding extensions, and experimental validation on hardware platforms.

References

- [1] F. Liu et al., ”Integrated Sensing and Communications: Toward Dual-Functional Wireless Networks for 6G and Beyond,” *IEEE J. Sel. Areas Commun.*, vol. 40, no. 6, pp. 1728–1767, 2022.

- [2] R. Mahmoud et al., "Sensing-Assisted Communication for mmWave Networks: A Review of Techniques, Applications, and Future Directions," *Electronics*, vol. 14, no. 19, 2025.
- [3] D. d. S. Brillhante et. al., "A Literature Survey on AI-Aided Beamforming and Beam Management for 5G and 6G Systems," *Sensors*, vol. 23, no. 9, 2023.
- [4] A. M. Nazar et al., "ENWAR 2.0: An Agentic Multimodal Wireless LLM Framework with Reasoning, Situation-Aware Explainability and Beam Tracking," *IEEE Trans. Mobile Comput.*, pp. 1–18, 2025.
- [5] Y. Zeng, Q. Wu, and R. Zhang, "Accessing From the Sky: A Tutorial on UAV Communications for 5G and Beyond," *Proc. IEEE*, vol. 107, no. 12, pp. 2327–2375, 2019.
- [6] C. Yanpeng et al., "Sensing-assisted Accurate and Fast Beam Management for Cellular-connected mmWave UAV Network," *China Commun.*, vol. 21, no. 6, pp. 271–289, 2024.
- [7] A. M. Benaya et al., "Aerial ISAC: A HAPS-Assisted Integrated Sensing, Communications and Computing Framework for Enhanced Coverage and Security," *IEEE Trans. Green Commun. Netw.*, vol. 9, no. 4, pp. 2101–2114, 2025.
- [8] S. Zhou et al., "Temporal-Assisted Beamforming and Trajectory Prediction in Sensing-Enabled UAV Communications," *IEEE Trans. Commun.*, vol. 73, no. 7, pp. 5408–5419, 2025.
- [9] X. Zhang, M. Peng, and C. Liu, "Sensing-Assisted Beamforming and Trajectory Design for UAV-Enabled Networks," *IEEE Trans. Veh. Technol.*, vol. 73, no. 3, pp. 3804–3819, 2024.
- [10] W. Chen et al., "Sensing-Assisted Beam Tracking with Real-Time Beamwidth Adaptation for THz Communications," 2024. [Online]. Available: <https://arxiv.org/abs/2411.08264>
- [11] Q. Ziao and Y. Haifan, "A Review of Codebooks For CSI Feedback in 5G New Radio and Beyond," *China Commun.*, vol. 22, no. 2, pp. 112–127, 2025.
- [12] C. Liu et al., "Millimeter Wave Beam Alignment: Large Deviations Analysis and Design Insights," *IEEE Journal on Selected Areas in Communications*, vol. 35, no. 7, pp. 1619–1631, 2017.
- [13] J. M. Romero-Jerez and F. J. Lopez-Martinez, "On the distribution of the squared norm of non-circular complex Gaussian random variables with applications," in 2015 IEEE International Symposium on Information Theory (ISIT), 2015, pp. 341–345.
- [14] U. T. Demir, E. Bjornson, and L. Sanguinetti, "Foundations of User-Centric Cell-Free Massive MIMO," *Foundations and Trends in Signal Processing*, vol. 14, no. 3–4, p. 162–472, Jan. 2021.